A STUDY OF THE DISCHARGE CHARACTERISTICS OF LEAD–ACID BATTERIES*

P. HORVÁTH, Mrs P. JEDLOVSZKY and M. BENEDEK

Research Institute of the Electrical Industry, Budapest XV, Cservenka Miklós út 86 (Hungary)

(Received July 10, 1981; in revised form March 2, 1982)

Summary

A theoretical analysis of the electrolyte concentration distribution and current distribution in the porous lead dioxide electrode has been made by application of Fick's second law which was combined with approximate mass balances. The macrohomogeneous model for porous electrodes was used. The parameters in the models were determined experimentally for the lead dioxide battery plates and the special experimental cylindrical electrodes investigated. Numerical solutions for special cases are discussed. Theoretical results are in good agreement with experimental determinations. According to laser interferometry analysis the assumption of convectionless diffusion is, in practice, a good approximation in most cases.

Theoretical studies of the local overpotential show that the utilizable capacity is determined by the decreasing ionic concentration of the electrolyte because the electrode reaction takes place mainly in the outer layers of the electrode, if the discharge current has a high value, *e.g.*, full discharge time is less than 10 min.

Introduction

The characteristics of porous battery electrodes are mainly determined by reactant depletion and current distribution. Construction and optimization of porous electrodes must be based on a model able to predict how these phenomena influence the discharge characteristics. During the last two decades various mathematical models have been published in this area for the theoretical treatment of electrode reactions in porous media [1, 2] and applications of these models have been made to practical electrodes [3 - 12]. In the case of the very important lead dioxide electrode used as positive electrode in the lead–acid battery, theoretical and experimental investigations of current distribution, electrolyte depletion, and so called local passivation have been made [3, 7, 8]. The investigations have given contradictory results because their initial assumptions have not taken into account all the characteristics involved.

*Paper presented at the 2nd Czechoslovak International Conference on Electrochemical Power Sources, Žilina, Czechoslovakia, June 22 - 26, 1981.

0378-7753/82/0000-0000/$02.75

The purpose of the present paper is to outline the components of the local overpotential of the porous lead dioxide electrode in sulfuric acid solution, the current and overpotential distribution in it, the change of specific resistivity of the positive active mass, and the influence of these characteristics on the discharge behaviour of the battery. The role of the structure and shape of the separators used between the positive and negative electrodes has been taken into account.

By the application of Fick's second law with modified transport coefficients, a simplified theory of the positive plate of the lead–acid battery in the case of extremely high rates of discharge has been described by Stein [5]. The calculated discharge capacity of the investigated plates was lower than the measured value. Calculations were made by Lehning [6] on the same mathematical basis in the range of medium discharge rates, taking into account the sulfuric acid solution in the 2 mm space between the positive and negative plates of an SLI battery. The theoretical and experimental discharge curves gave contradictory results. In an attempt to explain this problem, the electrode polarization was increased by an amount corresponding to the ohmic potential drop in the so-called inactivated layer of low porosity occurring on the outer electrode surface at the end of discharge.

This concept has been used by Micka and Rousar [7, 8] under the same circumstances in the most recent complex theoretical treatments of this area. The macrohomogeneous electrode model was used, represented by the superposition of two continuous media, solid and liquid. Sulfuric acid was considered as a binary 1:1 electrolyte. The porosity of the electrode depends on the coordinate perpendicular to the electrode surface. The electrical conductivity of the solid phase positive active mass was assumed to be high so that its ohmic potential drop could be neglected. For obvious reasons the increasing effect of electrode polarization could not be taken into account in their theory [8]. Therefore, the time at which "the plate surface becomes inactive" in their *ad hoc* interpretation, was regarded as the end of discharge.

The present work deals with the determination and numerical solution of the differential equations derived by Stein [5] and Lehning [6] describing the mass transport in the electrolyte, combined with the local change in the electrode porosity connecting the local conversion of lead dioxide into lead sulphate according to the consumption of electricity [5]. The current distribution can easily be obtained in the simplified case of uniform or "slightly" changing concentration, porosity, and specific surface, corresponding to the initial moments of discharge, or when the numerical solution of equations could follow its change during discharge.

Concentration distribution and current distribution

The basic differential equation for the concentration distribution in the porous structure of an electrode is given by [5, 6]:

$$\frac{\partial c}{\partial t} = \left\{ f_i(c)\sigma \frac{\partial U}{\partial c} + D(c) \right\} \frac{\partial^2 c}{\partial x^2} + \left\{ \frac{\partial D(c)}{\partial c} + f_i(c) \frac{\partial}{\partial c} \left(\sigma \frac{\partial U}{\partial c} \right) \right\} \left(\frac{\partial c}{\partial x} \right)^2 . \tag{1}$$

One of the boundary conditions is connected with the requirement for continuity of the electrolyte concentration on the electrode and electrolyte surface. The other is concerned with the mass balance and will be given an equation related to the concentration gradients on the inner and outer sides of the electrode surface.

It will be understood, as stated above, that the current distribution is governed by the following two equations [1 - 3]:

$$\begin{aligned} \operatorname{div} i_2 = \frac{\mathrm{d}i_2}{\mathrm{d}x} &= - f_0 i_0 \exp\left(- \frac{\eta}{\eta_0} \right) \\ \frac{\mathrm{d}\eta}{\mathrm{d}x} &= \frac{\sigma_1 + \sigma_2}{\sigma_1 \cdot \sigma_2} i_2 - \frac{I}{\sigma_1} . \end{aligned} \tag{2}$$

The first equation gives the actual electrochemical kinetic expression between i_2 and η, while the second gives the origin of the change of the overpotential inside the pore.

Before the current distribution, the concentration distribution and the time dependent overpotential values can be calculated from these equations, the actual values of the various parameters appearing in the equations above must be determined by suitable experimental methods.

Experimental methods for determining the parameters in the model

Determination of the polarizations

In the literature there have been many reports on the kinetics of the cathodic discharge of lead dioxide in sulphuric acid solution,

$$PbO_2(s) + 3H^+ + HSO_4^- = PbSO_4(s) + 2H_2O - 2e$$

and on the kinetics of the anodic discharge of lead into lead sulphate under the same conditions:

$$Pb(s) + HSO_4^{2-} = PbSO_4(s) + H^+ + 2e.$$

These reactions produce solid lead sulphate on the inner surface of the electrode, consume ionic sulphate from the solution, and result in a change of potentials in the actual electrodes and electrolyte arrangement. In addition to this change there will be another additive part of the overpotential, depending on the current density.

Fresh experiments have therefore been carried out with the limited purpose of determining the various components of the overpotential during full discharge. The experimental methods were as follows:

— galvanostatic discharge of a lead dioxide surface formed by anodic oxidation of a circular cross-section lead rod (99.99% grade) in sulphuric acid solution of concentration 0.5 - 6 mol/l, at 25 °C;

— a further control was carried out with a low porosity, thin lead dioxide surface formed by electrodeposition of lead dioxide on a smooth Pt–Pd surface from a solution of lead nitrate and nitric acid;

— galvanostatic discharge of a porous lead dioxide surface, thickness about 0.1 mm, produced on the basis of SLI-type battery technology;

— galvanostatic discharge of a lead surface formed by cyclic oxidation and reduction in a sulphuric acid solution.

The galvanostatic discharge was carried out at 25 ± 1.5 °C, and the electrode potentials were measured against a mercury–mercurous sulphate reference electrode with a digital voltmeter. The electrolyte concentration was measured by a calibrated pycnometer. The results are illustrated in Fig. 1 for the positive lead dioxide electrode and in Fig. 2 for the negative lead electrode as a function of the electrolyte concentrations.

The electrode potential, in various constant concentrations, was measured during full discharge as a function of the relative discharge capacity. These results are given in Fig. 3. It is easy to realize that under these circumstances, when the electrode is thin, the electrode potentials change by only a few millivolts in the up to 80 - 90 per cent. discharge range.

The overpotential was defined as the difference between the equilibrium open-circuit potential in the given electrolyte solution and the constant

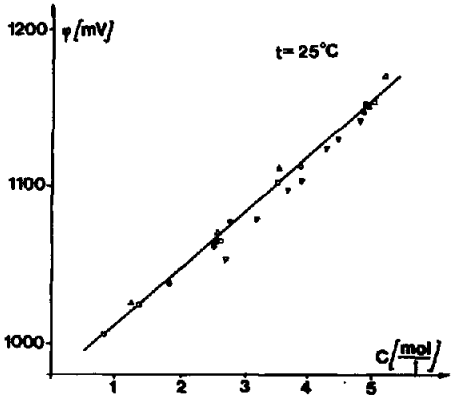

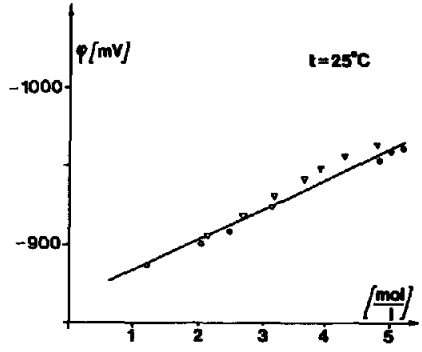

Fig. 1. The dependence of the potential of lead dioxide electrodes on the electrolyte concentration. ○, Formed on smooth lead; □, electrodeposited on Pt/Pb; △, electrodeposited on lead; ▽, industrial SLI electrode; $I = 5 \times 10^{-2} C_5$.

Fig. 2. The dependence of the potential of lead electrodes on the electrolyte concentration. ○, Formed on smooth lead; ▽, industrial SLI electrode; $I = 5 \times 10^{-2} C_5$.

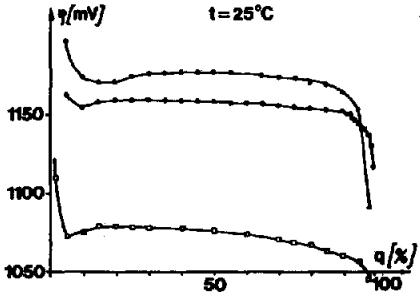

Fig. 3. The dependence of the potential of lead dioxide electrodes upon the relative discharge capacity. ●, Electrode formed in 5.25 mol/l concentration electrolyte; ○, electrodeposited in 4.75 mol/l electrolyte; □, formed in 2.55 mol/l electrolyte.

electrode potential obtained after the initial potential change at the beginning of discharge.

The current density was constant and the same value was applied in each case, so it could be categorically stated that the voltage drop was connected with the kinetics of charge transfer, and remained almost constant in every case measured. The behaviour of the potential was similar when other current densities were applied. The slope of the curves in Figs. 1 and 2 characterizes only the concentration dependence of the given electrode process.

According to these measurements, the overpotential of the positive electrode can be considered as three separate additive parts over a wide range of discharge current densities. One part is a linear function of the electrolyte concentration, the second depends exponentially on the local current density — its values were found to be approximately within the Tafel region (in most practical cases it is obtained when the current density is not less than 2 - 3 mA/cm^2; the other cases, from a practical point of view insignificant, have been examined in the literature [2, 11]).

According to the measured data the slope of the linear portion is 35 ± 3 mV l mol^{-1} in the case of the lead dioxide electrode when the concentration range is 0.6 - 6 mol/l at 25 °C, and 19 ± 3 mV l mol^{-1} for the lead–lead sulphate electrode reaction (Figs. 1 and 2).

The third component of overpotential depends on the local active material content at the end of discharge, as can be seen in Fig. 3. This dependence can be characterized experimentally by the effective conductivity of the solid porous electrode matrix, σ_1.

Determination of σ_1

Lead dioxide is a semiconductor with a high conductivity. The conductivity of a porous structure depends on the contacts between the particles. An exact determination of the effective conductivity of the porous electrode matrix was made by measuring the voltage drop across an electrode of special shape and known dimension cut from the electrode matrix, when d.c. of a known value was applied. For a fully charged specimen (after the

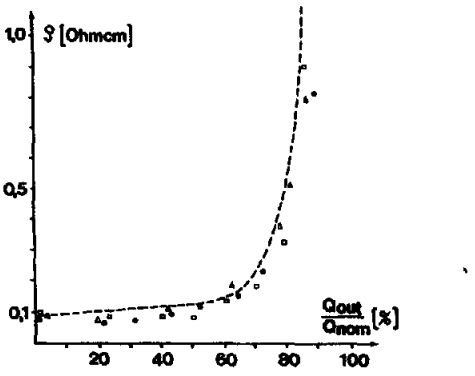

Fig. 4. The dependence of the effective specific resistivity on the relative discharge capacity. ○, $I = 0.1\ C_5$; □, $I = 0.16\ C_5$; △, $I = 0.5\ C_5$.

fifth formation cycle) and for a partly discharged specimen the conductivity was measured in the dry state. The effective resistivity, the reciprocal of the above mentioned effective conductivity, has been used to illustrate this graphically in Fig. 4. The specific resistivity of the porous positive active mass increases exponentially during discharge as a function of the relative discharge capacity. At the end of discharge it could reach 200 - 300 times the initial value. An empirical expression can be found to describe its dependence upon the relative discharge capacity, $x = Q_{out}/Q_{nom}$, as follows:

$$\rho(x) = \rho_0(1 + x) + \rho_0 \exp\,[16(x - 0.7)]\,. \qquad (3)$$

This empirical expression is shown in Fig. 4 as a dotted line. According to our working hypothesis, expression (3) also applies in local circumstances, so the electrode can be simulated by an electrical network of ohmic resistances equivalent to the ionic resistances of the electrolyte to be found in the porous structure as determined by Wiesener and coworkers [10], and the resistances of the porous electrode matrix determined from expression (3).

This network is illustrated in Fig. 5 for the positive lead dioxide electrode, where $R_{1,i}$ are the above mentioned local ionic resistances, $R_{2,i}$ are the resistances of the solid matrix, U_i is the sum of the overpotentials of the

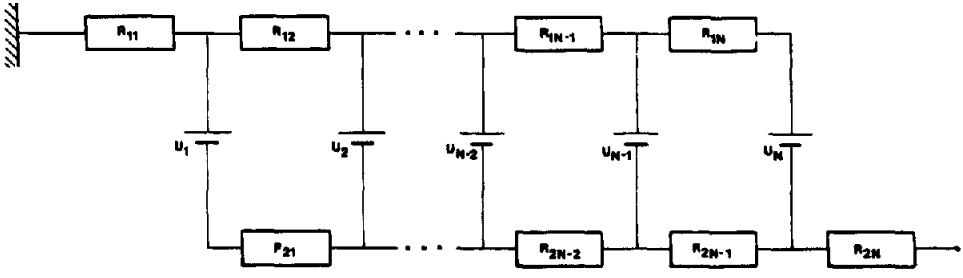

Fig. 5. The equivalent network of a positive porous lead dioxide electrode.

Tafel values (its slope is about 30 mV/decade) and the component values depend on the local electrolyte concentration as shown in Fig. 1.

Experimental investigation of the concentration profile

The method of laser interferometry was used to examine the electrolyte concentration profile. The principle of the measuring scheme is shown in Fig. 6. It is a three angle interferometer, where 1 is an argon ion laser, and 2 is a cuvette containing a 2.1 mm thick PbO_2 electrode of known surface area with a Pb electrode on either side and 6 mm distant from it. We examined the neighbourhood of the vertical positive electrode during discharge. The range of electrolyte concentration was 1.2 - 1.3 g/cm^2. The interference pictures were detected by a Javalin-type solid state camera (see ref. 3) and an oscilloscope-recording and analyzing system was used to arrive at the results which are illustrated in Fig. 7. The calculated results were confirmed by experimental values during the first 3 - 5 min. After this period the concentration profile reached a stable value at a distance of about 1.2 - 1.4 mm from the electrode surface in the case of a 1 cm high electrode. This can be explained, on the basis of Levich's work, as spontaneous convection near the surface. For a plate of practical dimensions the diffusion layer thickness will be about 2.6 mm according to calculation. The thickness of the separator rib is however, much less than 2.6 mm in practice and spontaneous convection will be strongly inhibited. For this reason the assumption of convectionless diffusion is a good approximation.

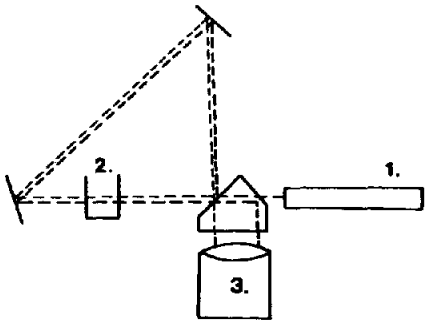

Fig. 6. Schematic diagram of the laser interferometer.

Theoretical analysis of the concentration and current distributions

The equations given above from the literature can now be applied to the lead–acid battery under investigation. Numerical solutions can be derived when all the coefficients are known in the differential equations. The conductivity of the free electrolyte, σ_1, was taken from tabulated values; the

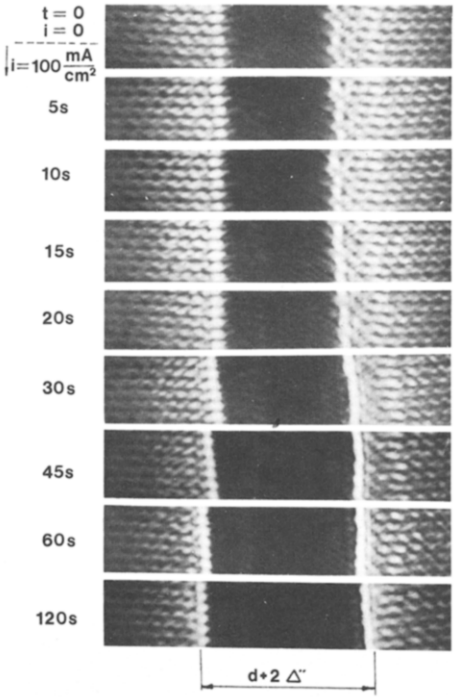

Fig. 7. Laser interferometry experimental results during discharge of a positive electrode.

values of D, the experimental diffusion coefficient of sulfuric acid solution in dependence on concentration at 18 °C were taken from refs. 7 and 8, and allowance was made for the fact that it increases by about 2% for each degree centigrade rise in temperature; the factors f_i connect the mass balances and electrolyte consumptions. The latter values were used by Stein [5] and Lehning [6]. The method of numerical solution of the equations consisted of reduction of the time derivatives by the Crank–Nicholson scheme [13] and substitution of the other derivatives by their first and second differences (see Appendix). The calculation of current and potential distribution was made by the Runge–Cutta method with regard to the boundary conditions at every step, after the actual concentration distribution was known. The numerical solution was performed on a TPAi-type computer and the programme was written in Fortran IV.

Results and discussion

The calculated concentration profiles in a real electrode–electrolyte arrangement are shown in Fig. 8. In this Figure the concentration profiles are shown from the geometric center of the negative electrode to the positive electrode. From the profiles it can be easily understood that the concentration changes only slightly in the region of the electrodes. The total

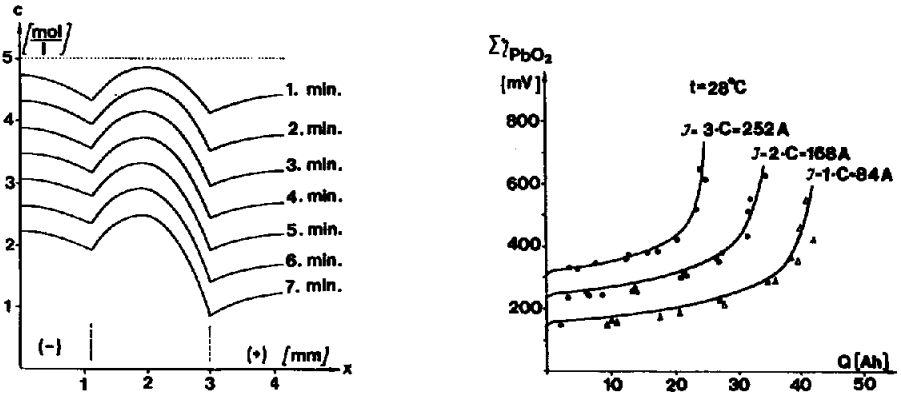

Fig. 8. The calculated concentration distributions of an SLI battery. I = 252 A, at 25 °C.

Fig. 9. The sum of the overpotentials of SLI batteries. The discrete points were measured, the full lines were calculated.

overpotential is shown as a function of the discharged capacity at given current in Fig. 9. The full lines show the calculated values and the discrete points are the measured values on the basis of 18 separate experiments.

The calculated divergences of current density are shown in Fig. 10. The calculations were made for a VBKM 3 DN 6 type (made in Hungary) SLI battery. From these results it can be seen that the utilizable capacity is determined particularly by the decrease of the ionic concentration of the electrolyte within the pores of positive electrodes in actual cases when the discharge current has a high value, *e.g.*, full discharge time is less than 10 min. In other cases or when the electrolyte is in excess, the current distributions and the utilizable capacity are determined mainly by the effective conductivity of the active mass.

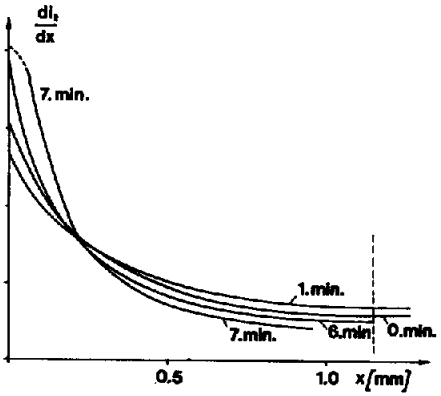

Fig. 10. The calculated values of the divergence of the current density. I = 252 A, at 25 °C.

Conclusions

According to these results the assumption of constant concentration in the calculation of the current distribution is a good approximation. For an exact description of the behaviour of the electrochemical processes occurring during discharge, the local change in the active material must be taken into account. According to our examination and experimental results the change in the effective conductivity of the active matrix is a positive function of the discharged capacity. Construction and optimization of the porous electrodes, mainly for high rate batteries, can be undertaken from our complex mathematical model without the need for difficult, time consuming experimental work.

List of symbols

C	Concentration (mol/l)
D	Experimental diffusion coefficient of sulphuric acid
i_2	Current density in the pore electrolyte
η	The electrode potential as a function of the coordinate perpendicular to the electrode surface
σ_1	Effective conductivity of the electrode matrix
σ_2	Effective conductivity of the pore electrolyte
I	Total current density in the bulk electrolyte
f_0	The specific surface area
η_0	An empirical value of the Tafel slope, calculated from the polarization curve [3]
R_{1i}	Local ionic resistances
R_{2i}	Resistances of the solid matrix
U_i	Sum of the overpotentials of the Tafel values
Q_{out}	Relative discharge capacity
Q_{nom}	Nominal capacity

References

1 J. S. Newman and Ch. W. Tobias, *J. Electrochem. Soc.*, *109* (1962) 1183.
2 K. Micka, *Fuel Cell Systems*, American Chemical Society, Washington, 1965, p. 73.
3 D. Simonsson, *J. Electrochem. Soc.*, *120* (1973) 151.
4 K. J. Euler, *Electrochim. Acta*, *13* (1968) 1533.
5 W. Stein, *Dissertation*, Techn. Hochschule, Aachen, 1959.
6 H. Lehning, *Electrotechn. Zh., A*, *93* (1972) 62.
7 K. Micka and I. Rousar, *Coll. Czech. Chem. Commun.*, *40* (1975) 921.
8 K. Micka and I. Rousar, *Electrochim. Acta*, *18* (1973) 629; *21* (1976) 599.
9 P. Reinhardt, M. Voght and K. Wiesener, *J. Power Sources*, *1* (1976/77) 127.
10 K. Wiesener and G. Jürgen, in J. Thompson (ed.), *Power Sources 7*, Academic Press, London, 1979, p. 17.
11 E. A. Grens and C. W. Tobias, *Electrochim. Acta*, *10* (1965) 761.
12 K. Micka and M. Svatá, *J. Power Sources*, *4* (1979) 43.
13 J. Crank and L. T. Nicholson, *Proc. Camb. Philos. Soc.*, *43* (1947) 50 - 67.

Appendix

Electrode models and derivation of general equations

For the case where we assume the transport of mass and electricity without convection the basic equation is:

$$\frac{\partial C_i}{\partial t} = -\nabla N_i - \delta_i \tag{A1}$$

where C_i denotes the concentration of species i in mol/l of solution, N_i the flux of species i (mol/dm^2 s) and δ_i the rate of consumption of species i (mol/l s).

For modeling a lead–acid cell we assume that the cell consists of two plates, one positive and the other negative with an electrolyte space between them. (The electrodes have a thickness $2d_p$ in the case of the positive plate and $2d_n$ in the case of the negative plate, and are polarised from both sides. Consequently, the plate-shaped electrodes of thickness d_i are polarised from one side, and the mathematical formulation is the same in both cases for reasons of symmetry [7].) The concentration of electrolyte is represented as c and depends on the coordinate, x, and the time, t, except for the initial value, C_0. The x axis is perpendicular to the surface of the electrodes; $x = 0$ corresponds to the geometric center of the positive electrode, $x = d_p$ to the positive electrode surface, $x = x_1$ to the negative electrode surface, and $x = x_2$ to the center of the negative electrode, for electrodes which are polarised from both sides. The porosities of the electrodes are denoted as p_p and p_n, respectively, and depend on the coordinates, x, and time, t, connecting the local conversion of the active mass into lead sulfate. The electrodes are loaded with a constant current density, I (A/cm^2).

Using phenomenological expressions, on the basis of the transport equations, the differential equation for the concentration distribution in the porous structure of electrodes can be obtained [5, 6]:

$$\frac{\partial c_i}{\partial t} = \left\{ f_i(c)\sigma \frac{\partial U}{\partial c} + D(c) \right\} \frac{\partial^2 c_i}{\partial x^2} + \left\{ \frac{\partial D(c)}{\partial c} + f_i(c) \frac{\partial}{\partial c} \left(\sigma \frac{\partial U}{\partial c} \right) \right\} \left\{ \frac{\partial c_i}{\partial x} \right\}^2 \tag{A2}$$

or

$$\frac{\partial c_i}{\partial t} = A_i(c) \frac{\partial^2 c_i}{\partial x} + B_i(c) \left(\frac{\partial c_i}{\partial x} \right)^2 \tag{A3}$$

where $f_i(c)$ denotes the consumption of acid in mol/A s; $f_n = 4.19$ mol/A s denotes the consumption of acid at the negative electrode, and $f_p = \{6.16 +$

$0.1865c\ (1/[1\ \text{mol/l} - 0.037c])\} \times 10^{-6}$ mol/A s denotes the empirical expression for the consumption of acid and production of water at the positive electrode on the basis of Stein and Lehning [5, 6]. $D(c)$ represents the experimental diffusion coefficient of sulphuric acid, and its dependence on c is approximately linear. The equation is $D = 1.48 \times 10^{-5}$ cm^2/s + $0.155 \times 10^{-5}\ c$ cm^2 l/mol s at 18 °C, and it increases by about 2% per degree centigrade. σ denotes the conductivity of sulphuric acid at 25 °C. The values were taken from the literature and were fitted to a parabola of the form

$$\sigma(c) = (-5.664 \times 10^{-2}\ \text{l}^2/\text{mol}^2 \times c^2 + 0.4204\ \text{l/mol} \times c + 4.197 \times \times 10^{-2})\ \text{ohm}^{-1}\ \text{cm}^{-1},\ \text{for}\ 0.5 \leqslant c \leqslant 6\ \text{mol/l}.$$

U denotes the difference between the potential of the solid phase, ϕ_1, and the liquid, ϕ_2.

One of the boundary conditions is connected to the requirement for continuity of the electrolyte concentration on the electrode–electrolyte interfaces. The other is followed by the mass balance and will be given an equation related to the concentration gradients on the inner and outer surfaces [6] of the negative and positive electrode–electrolyte interface:

$$\left.\frac{\partial c_i}{\partial x}\right|_{\text{inner}} = \frac{f_i(c)}{D(c) + \sigma \cdot f_i(c) \cdot \dfrac{\partial U}{\partial c}} \cdot p_i \left\{ I - \frac{D(c)}{f_i(c)} \left.\frac{\partial c}{\partial x}\right|_{\text{outer}} \right\} \tag{A4}$$

where the values of i = n, and p refer to the negative and positive electrode, respectively.

It is obvious that in eqn. (A3)

$$B_i(c) = \frac{\partial A_i(c)}{\partial c} + \Delta_i \tag{A5}$$

where $\Delta_i = 0$ in the case of the negative electrode and the bulk electrolyte between the electrodes. In the case of the positive electrode $\Delta_p \neq 0$, but in reality, $\Delta_p \equiv 0$ is a good approximation in this case also.

Equation (A2) shows non-linearity. This may be reduced to a simpler form by introducing the new variable:

$$\theta_i(c) = \int_0^c \frac{A_i(c)}{A_{i,c=0}}\, dc \tag{A6}$$

where the values of i = 0, 1, and 2, refer to the negative electrode, the bulk electrolyte and the positive electrode, respectively; and $A_{i,c=0}$ is the value of $A_i(c)$ when $c = 0$.

It follows from eqn. (A6) that the original differential equation (A2) becomes:

$$\frac{\partial \theta_i}{\partial t} = A_i(c) \frac{\partial^2 \theta_i}{\partial x^2} . \tag{A7}$$

Equations (A7) are 2nd order linear partial differential equations. This system, taking into account its boundary equations (which depend on the new integral transformed variables, θ_i), can be readily solved numerically by replacing the 2nd order partial derivatives with their corresponding 2nd order finite differences.

Suppose that we know the $\theta_{i,k}$ values of a function $\theta_i(x)$ at regular intervals ($0 \leqslant x_i^* \leqslant 1$, where x_i^* denotes the dimensionless parameters, $x_i^* = x/d_i)\Delta x^* = kh, k = 1,2, \ldots, N$, of its argument.

The equation to be solved for one of the space sections of interest is:

$$\frac{1}{A}\frac{\partial \theta}{\partial t} = \frac{\partial^2 \theta}{\partial x^2}$$

$$\theta(0,t) = \theta_1(t) \qquad \theta(1,t) = \theta_2(t) \qquad \theta(x,0) = \theta_0 \tag{A8}$$

$$\left.\frac{\partial \theta}{\partial x}\right|_{x=0} = G_1(t) \qquad \left.\frac{\partial \theta}{\partial x}\right|_{x=1} = G_2(t).$$

Replacing $\partial\theta^2/\partial x^2$ in eqn. (A8) by the 2nd difference and neglecting higher differences, gives

$$\frac{1}{A}\frac{d\theta_x}{dt} + \frac{-\theta_{k-1} + 2\theta_k - \theta_{k+1}}{h^2} = 0 \tag{A9}$$

$$k = 1, 2, \ldots, N-1.$$

In order to take into account the boundary conditions, the method may most simply be stated by introducing the set of concentrations θ_{-1} and θ_{N+1} at the fictitious points $x^* = -h$ and $x^* = +h$ from the left-hand and right-hand sides of the interval. If $\theta_{i,k}$ is known for $k = 1$, and $k = N-1$, $\theta_{i,-1}$ and $\theta_{i,N+1}$ are determined immediately. This gives:

$$\begin{aligned} \theta_{i,-1} &= \theta_{i,1} - 2hG_1 \\ \theta_{i,N+1} &= \theta_{N-1} + 2hG_2. \end{aligned} \tag{A10}$$

Thus, adding these values to eqn. (A9), we obtain the system of $(N+1)$ ordinary differential equations:

$$\frac{1}{A}\frac{d\theta_0}{dt} + \frac{2\theta_0 - 2\theta_1}{h^2} = -\frac{2G_1}{h}$$

$$\frac{1}{A}\frac{d\theta_k}{dt} + \frac{-\theta_{k-1} + 2\theta_k - \theta_{k+1}}{h^2} = 0 \qquad k = 1, 2, \ldots, N-1$$

$$\frac{1}{A}\frac{\mathrm{d}\theta_N}{\mathrm{d}t} + \frac{-2\theta_{N-1} + 2\theta_N}{h^2} = \frac{2G_2}{h} \,. \tag{A11}$$

In order to reach the final solutions we must carry out a normal time integration within a $t_j \leqslant t \leqslant t_{j+1}$ time interval followed by the always stable Crank–Nicholson scheme [13], which gives the following linear system of equations:

$$\begin{aligned}
&\frac{1+\mu}{\mu}\,\xi_0^{j+1} - \xi_1^{j+1} = \frac{1}{\mu}\,\theta_0^j - \frac{h}{2}\,(G_1^{j+1} + G_1^j) \\
&-\xi_{k-1}^{j+1} + \frac{2(1+\mu)}{\mu}\,\xi_k^{j+1} - \xi_{k+1}^{j+1} = \frac{2}{\mu}\,\theta_k^j \\
&-\xi_{N-1}^{j+1} + \frac{1+\mu}{\mu}\,\xi_N^{j+1} = \frac{1}{\mu}\,\theta_N^j + \frac{h}{2}\,(G_2^{j+1} + G_2^j)
\end{aligned} \tag{A12}$$

where

$$\begin{aligned}
\xi_k^{j+1} &= \frac{\theta_k^{j+1} + \theta_k^j}{2} \\
\mu &= \frac{A\Delta t}{h^2} = \frac{\tau}{h^2} \,.
\end{aligned} \tag{A13}$$

This system of equations contains $(N + 3)$ unknown variables. On eliminating G_1 from the system (A12), we obtain a boundary condition of the form: $G_1 = 0$ at the geometric center of the electrodes polarised from both sides, *i.e.*, there is no flux. The other equation is the boundary condition (A4), assuming that the outer gradient is known from the similar system of the other part of the cell. The coordinate axes for each plate and for the electrolyte bulk remain the same as before, *i.e.*, we now have three independent coordinate systems.

The program described for the calculation of the numerical solution of the linear system of equations for the individual plates and bulk electrolyte was put into the form of subroutines, which were solved exactly for every time step.

The current density distribution and the total amount of the overpotential were calculated on the basis of the network illustrated in Fig. 5, as the solution of a well-known system, for every time step.